A QM/MM Study of the Bergman Reaction of Dynemicin A in the Minor Groove of DNA

Tell Tuttle,[†] Elfi Kraka,[‡] Walter Thiel,*[,†] and Dieter Cremer*[,‡]

Max-Planck-Institut für Kohlenforschung, Kaiser-Wilhelm-Platz 1, D-45470, Mülheim an der Ruhr, Germany and Departments of Chemistry and Physics, University of the Pacific, 3601 Pacific Avenue, Stockton, California 95211-0110

Received: March 26, 2007; In Final Form: April 30, 2007

The Bergman cyclization of the natural enediyne dynemicin A in its triggered form (**2**) bound to the minor groove of DNA is compared with the corresponding reaction of its open isomer (**4**) utilizing QM/MM methodology. The two isomers are typical representatives of 10-membered cyclic (**2**) and acyclic (**4**) enediynes, which possess significantly different barriers for the Bergman reaction in the gas phase (**2**, 20.4 kcal/mol; **4**, 31.3 kcal/mol). In the case of the cyclic enediyne (**2**) the explicit consideration of environmental factors such as the receptor DNA, the solvent water, and charge neutralization by counterions has only minor effects on the energy profile of the cyclization reaction and the corresponding optimized structures when compared with the gas phase. The energetics of the reaction is predominantly determined by QM (electronic) effects. This makes it possible to replace the explicit description of the environment by an implicit one, thus avoiding costly QM/MM calculations and using instead a decoupled QM+MM approach. A conformationally driven hinge mechanism is identified for **2** that makes it possible for the ligand to adjust to the dimensions of the minor groove without significant energy loss. In the case of the acyclic enediyne **4** a QM/MM treatment is necessary to describe the Bergman cyclization in the minor groove. QM/MM corrects the cyclization barrier from 31.3 to 23.7 kcal/mol, which makes the reaction feasible under physiological conditions. The reduction of the barrier is a result of transition-state stabilization, which is caused by an increased dipole moment and hence stronger electrostatic interactions with the environment. In both cases the anionic charge of dynemicin A is largely shielded by water solvation and ion pair formation so that it does not significantly affect the energetics of the Bergman cyclization.

1. Introduction

Dynemicin A[1] **1** (Scheme 1) is a naturally occurring compound that has received considerable interest over the past 15 years due to its potential antitumor application. The compound is a member of the enediyne family of antibiotics, which cause cell death through irreversible oxidative strand scissions of DNA.[2,3] Despite the high cytotoxicity of **1**[2,3] its usefulness as a drug has not yet been realized due to its lack of specificity toward tumor cells. Thus, several synthetic attempts[4−7] have been made to modify dynemicin in order to achieve specificity toward tumor cells. However, currently this goal has not been achieved.

The present work is part of a long-term research initiative aimed at designing nontoxic dynemicins that can distinguish between normal and tumor cells. In the first part of this work the reactivity of **1** in connection with its exceptional biological activity was investigated,[8,9] which involved determination of the energetics of the triggering reaction leading from **1** to **2** and of the subsequent Bergman reaction of **2** yielding the biologically active singlet biradical **3-S** (Scheme 2). The biradical can abstract hydrogen from DNA to form the arene **5**, which results in strand scission. In the case of a slow H-abstraction reaction, **3-S** may also undergo a retro-Bergman reaction to yield the open enediyne **4**. For the purpose of assessing these alternatives, the thermodynamic and kinetic stabilities of **3-S** were investigated by calculating the relative enthalpy of the biradical and transition states **TS(2−3)** and **TS-(3−4)** (Scheme 2). It was demonstrated that the kinetic stability and H-abstraction ability are related to the S−T splitting of **3**, i.e., the energy difference between **3-S** and the associated triplet state **3-T**.[10−15]

All previous calculations were carried out for the gas phase utilizing a model derived from docking studies between the dynemicin and DNA. The preferred docking mode was investigated, and it was found that **1** becomes biologically active in

SCHEME 1: Atom Numbering and Ring Notation of Dynemicin 1[a]

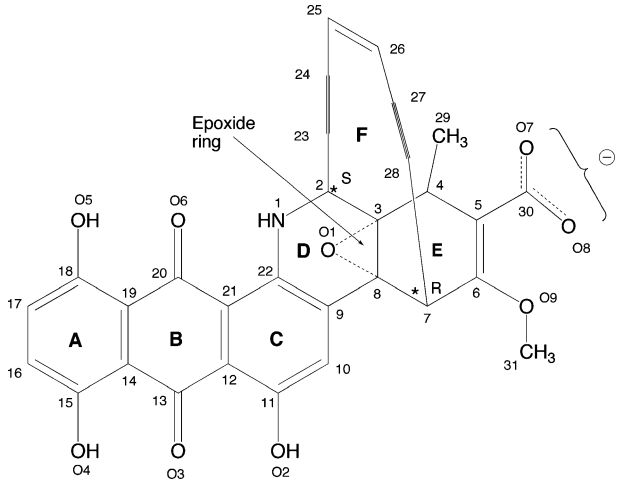

[a] Absolute configurations *R* or *S* are indicated for atoms C2 and C7.

* To whom correspondence should be addressed. E-mail: thiel@mpi-muelheim.mpg.de (W.T.), dcremer@pacific.edu (D.C.).
† Max-Planck-Institut für Kohlenforschung.
‡ University of the Pacific.

10.1021/jp072373t CCC: $37.00
Published on Web 06/22/2007

SCHEME 2: Reactivity of Dynemicin A (1) in DNA

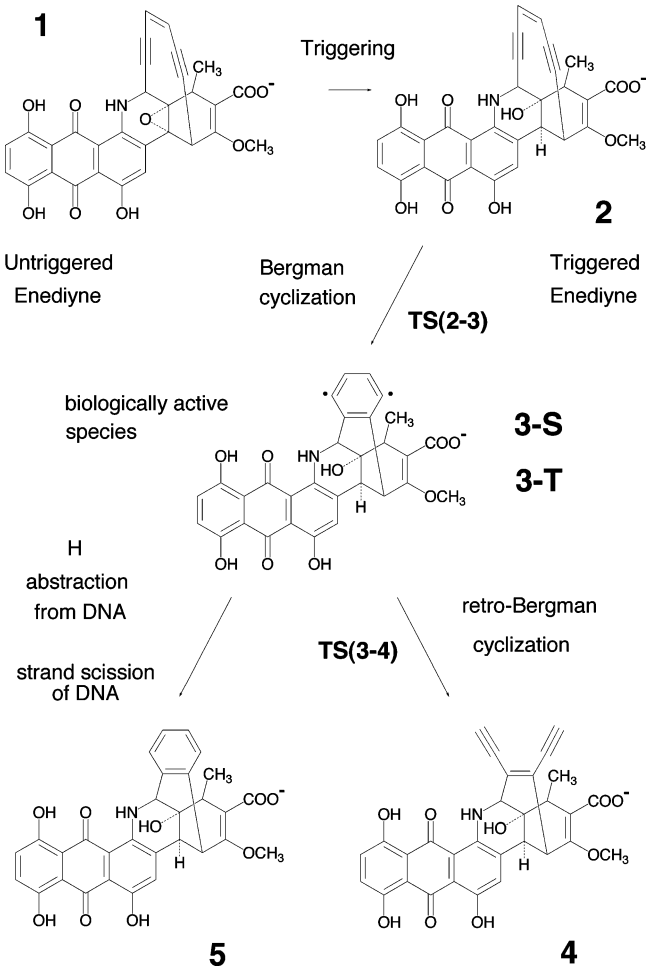

an insertion rather than intercalation mode, although the latter leads to a larger binding energy between **1** (or **2**) and DNA.[9] In the insertion mode the anthraquinone unit enters the minor grove edgewise (O2, O3, O4 first), with the ring system A−B−C being parallel to strands 1 and 2 (see Figure S1, Supporting Information) and the enediyne ring F about perpendicular to the strand direction. Hence, the triggering reaction, Bergman cyclization, and H-abstraction reaction take place when molecule **1**, **2**, or **3** (Scheme 2) is inserted rather than intercalated.

Rational drug design depends upon understanding how the drug interacts with the target receptor. The presence of the anthraquinone unit in dynemicin (Scheme 1) suggests that the compound binds to DNA via an intercalation mechanism,[16] and consequently, this binding mode was the focus of a number of computational[17−20] and experimental[4,21−27] studies. The possibility of an insertion mode of the ligand was never considered in these studies, although it explains the triggering of **1** and the regioselectivity of H abstraction by biradical **3-S**. The insertion model does not exclude the existence of an intercalation complex between **1** and DNA, which is indeed more stable than the insertion complex. However, it assigns the biological activity of dynemicin A to the formation of a precomplex, which involves the edgewise insertion rather than a direct intercalation of **1** into the minor groove of DNA.[9]

In view of the simplified model used in the previous study,[9] the findings have to be verified at a higher level of theory that includes the environment explicitly in the computational description. Since future investigations will focus on derivatives of **1** that will become biologically active only in the tumor cell rather than the normal cell, a reliable computational approach has to be established for the parent dynemicin. This is accomplished in the current investigation by employing QM/MM methodology, comparing its results with those obtained previously. We thus reinvestigate the Bergman reaction of **2** at the QM/MM level with its anionic form docked into the minor groove of the duplex 10-mer B-DNA sequence (CTACTACTGG)·(CCAGTAGTAG); the resulting DNA−dynemicin complex is solvated by water and neutralized by monovalent and divalent countercations.

The present paper is structured as follows. In section 2 a suitable QM/MM model is established and compared with the model used previously,[9] and the applied QM/MM methodology is briefly described. In section 3 the results obtained from the new model are presented and analyzed. Section 4 offers a summary and an outlook.

2. Models and Methods

A complete investigation of the Bergman reaction of **2** in the minor groove of DNA would require calculation of binding free energies ΔG_{bind} for **1**. However, such quantities are difficult to compute using QM/MM methodology. The large conformational changes associated with binding/unbinding of the ligand require extensive sampling of the conformational space. For example, when dynemicin docks into the minor groove a variety of processes will take place. (1) The docking process will loosen part of the solvent shell. (2) A rearrangement of the counterions will occur. (3) Conformational changes especially for the dynemicin side groups will occur. (4) The geometry of the minor groove of DNA may change to adjust to the shape of the drug. (5) A spline of water molecules will be partially or completely pressed out of the minor groove to provide a tighter fit for the drug. In addition, several different docking modes and docking positions need to be tested.[9] Sampling of this magnitude is still not feasible at a QM/MM level of theory, especially when taking into account that high-level QM methods would have to be applied for an accurate modeling of the noncovalent interactions between dynemicin and DNA.

In view of this situation we decided not to address the different binding modes in this QM/MM study (intercalation vs insertion) but to focus on the reactions of dynemicin A after its insertion into the minor groove of DNA. Using QM/MM methodology, it is nowadays possible to determine reaction free energies in large biomolecular systems provided that the reaction is essentially a local event (without large-scale conformational changes in the environment) and suitable approximations in the QM part are used (a comprehensive review and survey of currently available techniques has been recently published[28]). Experience with several enzymatic reactions indicates that such free-energy profiles are normally not dramatically different from the energy profiles obtained from optimization techniques. Thus, the latter approach is generally accepted as a useful tool in QM/MM studies of reactions in large biomolecular systems[28] and will consequently be used in the present work.

In our previous paper on **1**[9] we estimated the magnitude of free binding energies ΔG_{bind} and inhibition constants for the system DNA−dynemicin employing a simple model (henceforth called model A) based on the following assumptions. (1) Consideration of neutral **1** rather than its anion. (2) Modeling of DNA by the d(CTACTACTGG) dodecamer with a total charge of $-22e$. (3) Gas-phase optimization of the DNA fragment using MM methods. (4) Gas-phase optimization of neutral dynemicin A using DFT and a small basis set. (5) Use of a rigid docking protocol to place the ligand into DNA. (6)

Implicit consideration of the solvent via the AutoDock force field. (7) No consideration of counterions. (8) No energy minimization of the resulting complex. Because of simplifications 3−5 and 8 model A can be characterized as using an uncoupled QM+MM rather than the more advanced QM/MM methodology. Due to the neglect of counterions, model A uses the neutral rather than the anionic form of dynemicin so as not to exaggerate the electrostatic interactions with the polyanionic DNA fragment.[9] The primary assumption of model A is that the geometry of the complex obtained from rigid docking of gas-phase fragments would be sufficiently similar to the solution structure such that reasonable conclusions can be reached about the mode of interaction between ligand and receptor.[9] Moreover, model A does not consider entropic contributions explicitly but only takes them into account implicitly to some extent via the parametrization of the AutoDock force field,[29−31] which made it possible to obtain binding energies that are at least comparable (both in a qualitative and quantitative sense) to the experimental binding free energies of dynemicin and dynemicin analogues.[9] These simplifications complement the four essential mechanistic assumptions that underlie our recent studies of the docking modes of **1**.[9] (9) Dynemicin forms with DNA an insertion complex. (10) The drug is triggered and becomes biologically active in the insertion rather than the intercalation mode. (11) Free binding energies for insertion are smaller than those for intercalation, but trends in ΔG values are expected to be similar. (12) The docking process can be modeled by a single-docking rather than a multiple-docking mechanism.

Apart from simplifications 1−8 some methodological approximations in the QM and MM descriptions were also used. (a) The QM calculations were carried out with the 3-21G basis set[32] rather than the more costly 6-31G(d) or 6-31G(d,p) basis sets[33] employed initially.[10−15] This choice has been justified in our earlier gas-phase B3LYP[34−38] studies on **2**[8,9] with the 3-21G basis, which led to a reliable description of the energetics of the Bergman reaction[10,39] for the parent enediyne and several of its derivatives due to a fortuitous cancellation of basis set and correlation errors. Clearly, there is no proof that this will be also the case for dynemicins; however, all B3LYP/3-21G results obtained so far are consistent and in line with the observations made for small enediynes.[10−15] (b) The partial charges for the ligand and receptor were allocated with two different schemes due to the nature of the "peculiar" atom types that are present in ligand structures encountered along the Bergman cyclization path (e.g., biradical **3-S**, **TS(2−3)**, and **TS(3−4)**). Thus, different charge schemes were evaluated, and the combination of Mulliken charges for the ligand and Gasteiger−Hückel charges for DNA was found to provide a reasonable balance.[9] (c) The Amber force field[40] as implemented in HyperChem[41] was considered to be sufficient for minimizing the DNA dodecamer segment and obtaining a reasonable geometry and conformation. The duplex 10-mer B-DNA sequence d(CTACTACTGG)·d(CCAGTAGTAG) was chosen as a realistic model for docking because previous MM studies by others[20] had shown that the DNA region of interest is well conserved with a fragment length of greater than eight base pairs. (d) During the docking the ligand was kept rigid because of difficulties with the MM description of the enediyne structure (use of the generic force field in the docking program leads to a strongly destabilized ligand structure).

Using model A we obtained reasonable descriptions of **1** and **2** reacting inside the minor groove of DNA. Trends in binding free energies could be reproduced with the help of complexation energy differences, and the H atom to be abstracted could be correctly predicted.[9]

In this work we compare the results of model A with a new, QM/MM-based model B in order to identify those assumptions in the previous investigation that may lead to an unrealistic description of DNA−ligand interactions. On the other hand, if QM/MM theory can confirm the usefulness of model A within given application limits, then a firm methodological basis will be established from which the actual drug design work on nontoxic dynemicin can proceed with the use of the simpler model A.

Our QM/MM study of the aqueous system DNA−dynemicin also uses a rigid docking procedure to obtain a starting structure for **2**. However, apart from this, the QM/MM approach that defines model B is superior to model A with regard to the following. (I) Gas-phase optimization of anionic rather than neutral dynemicin. (II) Gas-phase minimization of the DNA fragment using the CHARMM force field,[42,43] which has been recently reparameterized for nucleic acid modeling.[44−46] (III) Solvation of the complete complex with TIP3P (transferable intermolecular potential with three parameters) water.[47] (IV) Neutralization of the system charge through inclusion of a suitable number of counterions. (V) Minimization of DNA, solvent, and counterions with dynemicin embedded into the DNA segment. (VI) Initial MD simulation to equilibrate the environment for building up a stable DNA−solvent−counterion configuration, again using the CHARMM force field. (VII) Hybrid QM/MM optimization of the equilibrated structure. (VIII) Hybrid QM/MM calculation of the full reaction profile of the Bergman cyclization of **2** in the minor groove of DNA.

In addition to the more accurate representation of the system with respect to the charge state of the ligand and the presence of the solvent and counterions, the QM/MM model also provides some clear methodological improvements. The QM/MM coupling scheme allows each region (QM and MM) to feel the presence of the other and adjust accordingly. Thus, while the first model makes use of a separate optimization of both the ligand and the receptor, the current model directly couples this optimization process such that a more realistic description of the effect of the environment on the Bergman cyclization can be evaluated. In this way, a detailed and reliable description of the different environmental effects that operate on the enediyne ligand during the Bergman cyclization of **2** can be given.

A complete description of the gas-phase calculations, system preparation, and MM calculations performed in this work can be found in the Supporting Information. Briefly, the QM/MM calculations were carried out at the (B3LYP/3-21G)/CHARMM level of theory, unless otherwise stated. The modular program package ChemShell[48,49] was used for all QM/MM calculations, where the QM energy and gradients were provided by Gaussian03.[50] ChemShell's internal force field driver using the CHARMM parameter and topology data provided the MM energy and gradients. The QM/MM coupling employed electrostatic embedding.[51]

The QM region contains the full dynemicin A ligand, resulting in 60 QM atoms. There is no covalent bond between the QM and MM regions and hence no need for a special treatment of the boundary region. For the QM/MM geometry optimizations a subset of the total system is optimized while the remainder of the atomic positions are frozen at the equilibrated geometry. The active subset for all optimizations was defined from the initial reactant complex geometry using a distance criterion, whereby any residue that contains an atom within 18 Å of any atom of dynemicin A is included in the active subset. The

TABLE 1: Comparison of the Energetics of the Bergman Reaction of the Anionic (A) and Neutral (N) Forms of Dynemicin 2 As Calculated with the 3-21G and 6-31+G(d,p) Basis Sets at the B3LYP Level of Theory[a]

		ΔE		$\Delta H(298)$		$\Delta G(298)$		μ	
structure	ref	A	N	A	N	A	N	A	N
2	**2**	0.0	0.0	0.0	0.0	0.0	0.0	15.0 (17.1)	4.4
TS(2−3)	**2**	20.4 (20.5)	19.4	18.5	17.6	19.6	19.0	14.7 (17.1)	4.2
3-S	**2**	−0.8 (−1.9)	−2.1	−1.4	−2.5	0.2	−1.0	15.0 (17.2)	5.0
3-T	**3-S**	2.8 (2.1)	2.8	3.1	3.1	2.4	2.3	15.0 (17.2)	5.0
TS(3−4)	**3-S**	23.0 (22.2)	22.4	20.8	20.3	20.2	20.0	14.8 (17.0)	5.4
4	**3-S**	−8.3 (−5.1)	−8.5	−9.0	−9.1	−11.4	−11.4	14.9 (17.1)	4.7
4	**2**	−9.1 (−7.0)	−10.5	−10.4	−11.6	−11.1	−12.4		

[a] Energies, enthalpies, and free energies are reported in kcal/mol (relative to the energy of a reference structure given in column 2) and dipole moments in Debye. B3LYP/6-31G+(d,p) results are given in parentheses. Geometries optimized at the B3LYP/3-21G and B3LYP/6-31G(d,p) levels of theory where the latter (see Supporting Information) are used for single-point B3LYP/6-31+G(d,p) calculations. Dipole moments were calculated using the standard orientation of the molecule.

resulting active region contains 2853 atoms, about one-quarter of the total system size (10 466 atoms). No electrostatic cutoff was applied for the QM/MM and MM/MM interactions. Further details of the QM/MM methodology employed are available in the Supporting Information

3. Results

Gas-Phase Calculations: Neutral vs Anionic Dynemicin A. At physiological pH, **2** and all its reaction products exist in an anionic state with the carboxylic acid substituent on ring E being deprotonated. Therefore, we re-evaluated the energetics of the Bergman cyclization of **2** using this anionic form in the gas phase to investigate whether inclusion of the negative charge affects the reaction profile (see Table 1). We previously established the usefulness of the 3-21G basis set in conjunction with the B3LYP functional in modeling the Bergman cyclization for naturally occurring compounds.[8,9] However, in all previous cases the systems under investigation were neutral species so that we need to check whether a larger basis set or inclusion of diffuse functions would significantly affect the results of the anionic species. The 6-31G(d,p)[33] and 6-31+G(d,p)[33,52] basis sets were chosen for this purpose.

There is little difference in the energetics of the Bergman reaction of **2** and the retro-Bergman reaction of **3-S** (see Scheme 2) when the neutral forms with the COOH group are converted into the anionic forms possessing the carboxylate group COO^-. The energy differences ΔE, enthalpy differences $\Delta H(298)$, and free energy differences $\Delta G(298)$ show deviations up to 1.3 kcal/mol from the corresponding values for the neutral species, where reaction barriers become slightly larger and reaction energies less exothermic.

The major change in the geometry of **2** upon ionization of the COOH group results from rearrangement of the H bonding with the neighboring methoxy group (Scheme 1). For the neutral form a H bond is established from COOH to the O atom of the methoxy group. This supports an outside bending of the methyl substituent. In the anion, however, the methyl group rotates inwardly to establish attractive $CH\cdots O^-$ interactions. The COO^- moiety is rotated out of the plane OC6C5C30 by 48° (132°) to allow for weak stabilizing interactions with the methyl group at C4.

The puckering analysis[9] of rings E and D reveals that the change in H bonding between the methoxy and COOH (COO^-) groups has no impact on the conformations of these two rings, which would in turn influence the conformation of the enediyne ring F (Scheme 1). In particular, there are no changes in the distances between the triple bonds, which are critical for the Bergman reaction, and it is thus understandable that the activation energy for the Bergman reaction is not affected by ionization of the COOH group. Hence, it is justified to model the Bergman reaction of **2** in the gas phase by investigating its neutral counterpart as done previously.[9]

TABLE 2: Analysis of the QM/MM Relative Energies (Model B) for the Bergman Cyclization of 2 As Calculated in the Minor Groove of DNA[a]

structure	ref	QM/MM	QM part	MM part	QM(gas)//QM/MM
TS(2−3)	**2**	21.0 (0.6)	19.3 (−1.1)	1.7	17.7 (−2.7)
3-S	**2**	−3.5 (−2.7)	−1.2 (−0.4)	−2.3	−3.5 (−2.7)
3-T	**3-S**	2.7 (−0.1)	2.7 (−0.1)	0	2.2 (−0.6)
TS(3−4)	**3-S**	18.0 (−5.0)	18.3 (−4.7)	−0.3	22.6 (−0.4)
4	**3-S**	−5.6 (2.7)	−8.5 (−0.2)	2.8	−5.2 (3.1)
4	**2**	−9.2 (−0.1)	−9.7 (−0.6)	0.6	−8.7 (0.4)
TS(3−4)	**4**	23.6 (−7.6)	26.8 (−4.5)	−3.1	27.8 (−3.5)

[a] Energies are reported in kcal/mol. Structures optimized at the B3LYP/3-21G//CHARMM level of theory. QM/MM is the relative energy of the total system. QM part is the relative energy of the QM subsystem in the field of the point charges from the MM subsystem. MM part is the relative energy of the MM subsystem which includes the vdW interactions with the QM subsystem. QM(gas)//QM/MM is the relative energy of the QM subsystem in the gas phase at QM/MM-optimized geometries. Values in parentheses provide the difference with respect to the relative energy from the gas-phase optimizations (Table 1).

Recalculation of the B3LYP/3-21G energetics at the B3LYP/6-31+G(d,p) level of theory leads to moderate changes in the energetics of the Bergman cyclization (Table 1, numbers in parentheses), the largest of which (2−3 kcal/mol) concern the relative stability of acyclic enediyne **4**. This confirms the usefulness of the 3-21G basis set in conjunction with the B3LYP functional for studying the reactions of the anionic form of dynemicin A (Scheme 2), as in the case of its neutral counterpart.[9] The B3LYP functional is preferred over the BLYP functional[35,36] because it suppresses significantly the self-interaction error of the Becke exchange functional,[53−58] which is important especially for the description of the singlet biradical **3-S** and the transition states **TS(2−3)** and **TS(3−4)**. Therefore, we apply B3LYP/3-21G also in the QM part of the QM/MM calculations.

QM/MM Optimizations: Influence of the Environment on the Bergman Reaction. Each of the stationary points along the reaction path **2** → **4** (Scheme 2) was optimized (for details of the optimization procedure, see the Supporting Information). Results of the calculations are summarized in Table 2.

With the exception of **TS(3−4)** involved in the ring-opening (closing) step **3-S** → **4** (**4** → **3-S**), the relative QM/MM energies are not significantly different from those calculated in the gas phase as reflected by the differences (values in parentheses) in Table 2. Inspection of the various components of the actual QM/

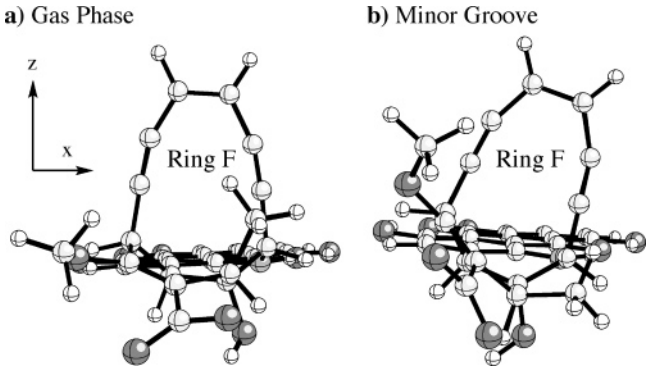

Figure 1. Tilting of ring F of **2** away from the backside of the minor groove: (a) gas-phase geometry (reference) and (b) minor-groove geometry. The backplane of the minor groove is in the minus *x* direction.

MM energy differences reveals that actually in each step along the reaction path small but significant energy changes occur for the interactions of the ligand with the environment, which however largely cancel each other.

For example, ligand **2** changes its geometry when docked into the minor groove in such a way that its energy increases, and consequently, the barrier for the first Bergman step is decreased by 2.7 kcal/mol to 17.7 kcal/mol (Table 2, entry QM(gas)//QM/MM, i.e., B3LYP/3-21G values calculated in the gas phase for the isolated ligand at its QM/MM geometry). This is due to a distortion of the ligand in the enediyne part (ring F) as shown in Figure 1. In the gas phase ring F is positioned perpendicular to the anthraquinone unit, tilted only slightly to the right (in positive *x* direction). When inserted into the minor groove ring F is tilted more strongly in positive *x* direction, thus being able to largely avoid steric repulsion with the backplane of the minor groove on the left side (Figure 1). This deformation is accompanied by a concerted clockwise rotation of the carboxy and methoxy groups positioned at ring E in a way that the methoxy group no longer sticks out toward the back of the minor groove (Figure 1). The bending of ring F outside the minor groove becomes possible by the flexibility of rings D and E that by appropriate puckering act together like a hinge mechanism. A second result of this deformation is a shortening of the distances between the triple bonds in ring F: 3.17 vs 2.97 Å and 2.71 vs 2.67 Å (gas phase vs minor groove). This facilitates bond formation across the ring and accordingly lowers the barrier to Bergman cyclization.

As mentioned, the reorientation of ring F requires a change in puckering of rings E and D. It was shown previously[9] that in the course of the Bergman cyclization ring E converts from a twist—boat form to a half-boat form with less puckering, which is supported by an appropriate adjustment of ring D to give the triple bonds a chance of approaching each other (see Supporting Information). Clearly, the QM/MM optimization moves **2** conformationally closer to **TS(2—3)** so that its energy is increased and the activation energy is decreased.

The reduction of the barrier is however counteracted by the polarization of the ligand through electrostatic interactions with the environment, as reflected by the QM part of the QM/MM energy (19.3 kcal/mol, an increase of 1.6 kcal/mol relative to the gas-phase value at the same geometry, i.e., Table 2, entry QM(gas)//QM/MM). In addition, environmental effects accounted for by the MM part (1.7 kcal/mol) lead to further destabilization so that in total the QM/MM activation energy for the Bergman cyclization is similar to the QM energy for the gas phase (0.6 kcal/mol higher, Table 2). The environment thus exerts opposing effects on the activation energy for the reaction **2** → **3** that largely cancel each other out.

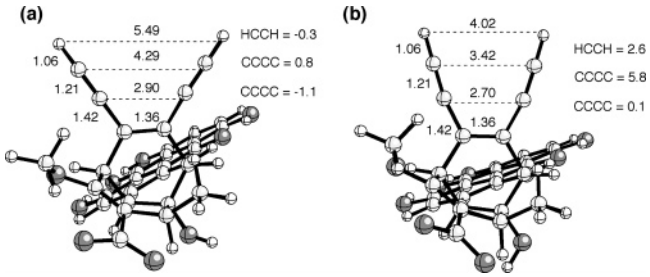

Figure 2. (a) Gas-phase and (b) minor-groove geometries of enediyne **4**. Distances in Ångstroms and dihedral angles in degrees.

The deformation of **2** during QM/MM optimization leads to a more exothermic reaction energy (changing by 2.7 kcal/mol from −0.8 to −3.5 kcal/mol, Table 2, entry QM(gas)//QM/MM), which is not altered by the sum of other effects. In the biradical **3**, the singlet—triplet splitting remains essentially unchanged because the environment affects the two spin states in the same way (Table 2). Overall, the previous use of model A[9] is thus well justified for the Bergman cyclization of **2** in light of the results obtained with model B. Qualitatively, the major effect of the environment is a reorientation of ring F, but the resulting changes in geometry and energy remain moderate, obviously because the minor groove provides enough space for a sideways insertion of **2** and for a low-energy hinge mechanism driven by appropriate ring puckering to reorient ring F.

The situation is however different for the Bergman reaction of the acyclic enediyne **4**, which in the gas phase has a barrier of 31.3 kcal/mol similar to that of the parent enediyne, (*Z*)-hex-3-ene-1,5-diyne (**6**).[10,12] The QM/MM activation energy however is just 23.6 kcal/mol, which after correcting for vibrational and thermal effects (about −2 kcal/mol[8,10]) should yield an activation enthalpy that makes the reaction possible at room temperature or under physiological conditions. Since this QM/MM result differs significantly from the previous prediction obtained with model A, it has to be clarified whether a change in the stability of enediyne **4** or **TS(3—4)** caused by the environment is responsible for the lowering of the activation energy.

It is well known that the barrier to Bergman cyclization can be reduced by incorporating the enediyne unit into a ring, thus decreasing the stability of the enediyne by ring strain, especially the angle bending strain of an alkyne unit that is forced to deviate from linearity. This strain is not felt in the TS because the triple bonds of the enediyne are in the process of converting to double bonds. These effects have been studied earlier at the CCSD(T) level for 9- or 10-membered cyclic enediynes.[14,15]

In the case of **4**, the calculated bending of the alkinyl groups caused by insertion into the minor groove is shown in Figure 2. The distances between the triple bonds of **4** are reduced from 2.90 to 2.70 Å and 4.29 to 3.42 Å (Figure 2). The data in Table 2, however, reveal that bending of the alkinyl groups has no significant effect on the stability of **4**, which shows a relief of ring strain of 9 kcal/mol (relative to **2**) no matter whether in the gas phase or in the minor groove. Hence, the reduced barrier to Bergman cyclization calculated for **4** when inserted into the minor groove results from a change in the stability of **TS(3—4)**.

Table 2 reveals that neither geometrical changes nor the MM part (van der Waals interactions of the ligand with the environment and changes in the environment itself) are responsible for the stabilization of **TS(3—4)**. This is mostly caused

by electrostatic interactions with the environment resulting from the fact that **TS(3−4)** possesses a dipole moment component in the *z* direction (direction of ring F, see Figure 1) 0.4 Debye larger than found for any of the other structures investigated along the reaction path. This becomes apparent when inspecting the dipole moments of neutral dynemicin, which are no longer disguised by the large influence of a negative charge (Table 1; **TS(3−4)** 5.4 vs 5.0 Debye for **3-S**; according to the chemical notation of dipole moments, the positive end of the calculated *z* component is the opening ring, the negative end the anthraquinone unit, Table 1). The increase in the dipole moment is a result of charge polarization upon ring opening and leads to stronger electrostatic interactions with the environment, thus lowering the energy of **TS(3−4)** by 4.7 + 0.3 = 5.0 kcal/mol (relative to **3-S**). This effect is enhanced by a destabilization of **4** by 2.7 kcal/mol (Table 2) so that a total barrier lowering of 7.7 kcal/mol from 31.3 to 23.6 kcal/mol results (Tables 1 and 2).

The energy barrier for the forward reaction from **3-S** → **4** is reduced by 5 kcal/mol from 23 kcal/mol in the gas phase to 18 kcal/mol in the minor groove. This reduction can become chemically relevant for substituted dynemicins with relatively low gas-phase barriers because in such a case the kinetic stability of intermediate biradical **3-S** could become too small, thereby hindering H abstraction and by this any biological activity.

Hence, the QM/MM investigation has brought about three important results. (a) The barrier to Bergman cyclization of an acyclic enediyne can be considerably reduced in the minor groove. (b) The cause of the barrier reduction is a stabilization of the TS by environmental effects rather than a destabilization of the acyclic enediyne caused by the bending of its alkyne groups. (c) In contrast to our earlier study, in which the docking of the gas-phase-optimized structure **4** into the minor groove of DNA turned out to be impossible for a rigid docking protocol (model A),[9] the QM/MM optimization of **4** reveals that the adjustment of the acyclic enediyne part to the minor groove is feasible at low energy cost.

Analysis of Interaction Energies between Ligand and Environment. As mentioned above, the changes in the QM region, i.e., the electronic structure changes, are the dominant effects that largely determine the QM/MM reaction profile. The contributions of the environment to the QM/MM energy have been discussed so far; however, their nature deserves closer inspection. We therefore performed an energy partitioning analysis that is described in detail in the Supporting Information. Here, the most significant observations and conclusions are summarized.

Bulk Environment Interactions. The MM energy differences given in Table 2 can be partitioned with respect to the three segments—water, DNA, and counterions—which comprise the environment. In addition, the MM component of the interaction energy between the ligand (QM) and each of these segments can be analyzed to determine the corresponding van der Waals (vdW) interactions (the electrostatic interactions are contained within the QM energy term, see below). The computed changes in the various interaction energies for a given step along the reaction path from one stationary point to the next are all relatively small (see Supporting Information, Table S2), and therefore, it is sufficient to point out just some general trends. (1) Since the global shape of the ligand, once inserted in the minor groove, does not change very much during the reaction sequence **2** → **4** the vdW interactions between DNA and ligand are almost constant. (2) Variations in the ligand−water and ligand−counterion interactions have to be negligible because these interactions are charge (H bonding) rather than van der Waals driven. The only notable change occurs during formation of enediyne **4** for the ligand−water vdW interaction, which becomes slightly less favorable due to ring opening. (3) DNA is relatively stiff and hardly distorted by the rearrangement of the inserted ligand as confirmed by the small changes in the DNA−DNA values. (4) The solvated counterions are far away from the reaction center so that they respond relatively little to changes in the ligand structure. Hence, changes in ligand−ion, water−ion, DNA−ion, and ion−ion interactions are also relatively small. (5) Sensitive measures for changes in the minor groove are provided by the water−DNA interactions. The water sphere is able to accommodate these changes such that the energetic consequences of the DNA−water interactions are balanced. This also involves the water−ion interactions. The breakdown of the calculated MM energy differences reveals this phenomenon.

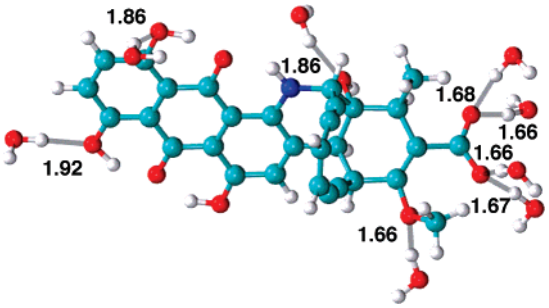

Figure 3. H-Bond network between **2** and water molecules. Distances in Ångstroms.

In general, changes in the environment of the ligand tend to compensate each other. Since the reaction considered leads from one enediyne to another the sum of all MM changes for the reaction **2** → **4** is close to zero but positive (destabilizing) because of the large hydrophobic part of the ligand.

Electrostatic Interactions Between Selected Residues and the Ligand. Individual interaction energies are listed and discussed in the Supporting Information. They confirm that the total electrostatic interaction of the anionic ligand is strongly repulsive with DNA and strongly attractive with the counterions where the latter effect dominates. Proceeding along the reaction path these electrostatic interactions become progressively less favorable overall (up to 4 kcal/mol) due to a stronger weight of the repulsive interactions with DNA strand 1. This is a result of increased Coulombic repulsion between DNA and ligand caused by the enhanced space demand of the acyclic enediyne unit in **4**. One should emphasize, however, that these variations remain minor (less than 3%) compared with the total electrostatic interaction energies.

H Bonding. The analysis of the electrostatic interactions between ligand and water molecules in the primary solvent shell (i.e., within 4 Å of the ligand) shows (see Supporting Information) that the sum of these energies does not vary much along the reaction path (by <1.7 kcal/mol). Obviously, the H-bond pattern in the primary shell does not change significantly. Figure 3 depicts the most important H bonds formed by the ligand.

The carboxylate substituent of the ligand is well solvated in the QM/MM description. There are four water molecules with H bonds to the oxygen atoms (O7 and O8) of the carboxylate, which acts as the acceptor. All four water molecules are strongly bound with an average H-bond length of 1.67 Å, and this connectivity is maintained along the reaction path. The closest potential H bond between the carboxylate and DNA would involve the H4′ atom of G7 at a distance of ca. 2.9 Å. In the

optimized gas-phase structure of **2** the carboxylate and methoxy substituents are oriented such that there is an attractive intramolecular interaction between the carboxylate and the H atoms attached to the methoxy C31 (see Scheme 1). This orientation is retained in the DNA environment because it does not hinder formation of four strong carboxylate/water H bonds and allows formation of another strong methoxy/water H bond involving the oxygen atom (O9) of the methoxy group (see Figure 3).

The oxygen atom (O1) from the epoxide ring of **2** (see Scheme 1) also forms a strong H bond to a water molecule. Moreover, there are weaker H bonds involving the hydroxy oxygen atoms of ring A (O4 and O5). All these H bonds remain conserved during the entire reaction, and judging from the H-bond lengths, their strengths remain about the same, except for the (weak) H bond involving the O5 atom, which points out of the minor groove and varies by about 0.1 Å during the course of the reaction (**2**, 1.86 Å, **3**, 1.77 Å).

Overall, the preceding analysis shows that there are no pronounced environmental effects on the energy profile of the rearrangement **2** → **4** with the exception of the ring opening to enediyne **4.**

4. Summary and Conclusions

The QM/MM investigation of the Bergman cyclization of **2** in the minor groove of DNA has led to several chemically important results.

(1) Acyclic enediynes can undergo the Bergman cyclization in the minor groove with a strongly reduced barrier compared to the gas phase. In the case of enediyne **4** the barrier is lowered by 7.6 kcal/mol from 31.3 to 23.7 kcal/mol, thereby being sufficiently reactive at room temperature. This was previously not known and opens the possibility of using acyclic enediynes if properly anchored in the minor groove for drug design.

(2) The dominant reason for barrier lowering is a dipole-driven stabilization of the corresponding transition state (in the example investigated **TS(3**—**4)**). An increase in the *z* component pointing in the direction of the breaking bond makes a stronger stabilizing electrostatic interaction of enediyne ligand and environment possible. This presents a new barrier lowering mechanism, which has to be separated from the strain-driven mechanism of barrier lowering so far mostly considered, which in the case of **4** plays only a minor role.

(3) Previous quantum chemical investigations of acyclic enediynes undergoing the Bergman reaction have been carried out mainly just for the gas phase. This does not represent the situation in the minor groove in cases as the one described, which need to be investigated by QM/MM methods (model B) explicitly considering the environment of the ligand in order to obtain a reliable description of the energetics of the reaction.

(4) For cyclic enediynes such as **2** environmental effects are found to largely compensate each other along the reaction path of the Bergman cyclization. Therefore, computational costs can be reduced using the QM+MM-based model A.

(5) However, even in the case of cyclic enediynes such as **2**, a QM/MM protocol is recommended to determine mechanistic details of the Bergman reaction proceeding in the minor groove, which cannot be observed in the gas phase. In this connection we report a puckering-driven (rings E and D) hinge mechanism that makes it possible for the enediyne ring F to bend out of the minor groove, thus lowering destabilizing steric repulsion and increasing stabilizing electrostatic interactions. A similar observation can be made for a protruding methoxy group that is moved out of the region of strong steric repulsion by a concerted rotation mechanism involving the carboxy group at ring E.

Apart from the chemical insights gained in this work, we obtained answers to questions concerning the appropriate computational description of DNA—ligand systems, especially the DNA—enediyne system.

(a) The use of neutral or anionic **2** leads to little changes in the energetics of the Bergman cyclization of dynemicin docked to DNA. This is the result of a mechanism that shields the negative charge of the carboxy group by intra- and intermolecular H bonding not changing during the reaction and complemented in form of a solvent-separated ion pair (separation distance 8 Å, twice the size of a reasonable solvation radius). There is no significant change in the energetics depending on the charge of the ligand. One may thus expect that proper shielding of the negative charge will also facilitate insertion of anionic **2** into the minor groove, in spite of the polyanionic character of DNA.

(b) We were able to establish in this work two useful modeling protocols. Model A will be the appropriate choice in all cases where environmental effects cancel each other largely so that the more costly model B can be avoided. This observation opens up the possibility of investigating a large number of dynemicin A analogues in connection with our drug design objectives just using model A. However, there will be always the need to apply the more complete QM/MM methodology if more reliable and detailed descriptions are required. QM/MM and model B become absolutely necessary when electronic and structural changes of the ligand occur in the minor groove, as is the case for acyclic enediynes.

(c) We were able to systematize the analysis of DNA—ligand interactions in a way that can be routinely applied. Such analysis offers the opportunity to identify crucial specific interactions and hence the physical source of special mechanistic effects.

Finally, we emphasize the need to further develop the methodology of investigating DNA—ligand interactions with computational means. One obvious aim is to clarify whether the binding of dynemicin is purely stochastic or follows some distinctive mechanism. In the present work, we concentrated on a single docking mode and did not address the relative ease of intercalation and insertion. This issue and the effect of multiple binding sites being occupied remain to be explored, in particular in the context of the question whether multiple docking will increase the flexibility of the DNA helix to such an extent that insertion and intercalation become competitive. Future investigations will have to consider these issues.

Acknowledgment. E.K. and D.C. thank the University of the Pacific for research support.

Supporting Information Available: Material describing the setup and preparation of the system as well as a detailed list of the electrostatic interactions are provided (PDF file) and final optimized structures (PDB file). This material is available free of charge via the Internet at http://pubs.acs.org.

References and Notes

(1) Konishi, M.; Ohkuma, H.; Matsumoto, K.; Tsuno, T.; Kamei, H.; Miyaki, T.; Oki, T.; Kawaguchi, H.; Vanduyne, G. D.; Clardy, J. *J. Antibiot.* **1989**, *42*, 1449.

(2) *Enediyne Antibiotics as Antitumor Agents*; Borders, D. B., Doyle, T. W., Eds.; Marcel Decker: New York, 1995.

(3) Konishi, M.; Toshikazu, O. In *Enediyne Antibiotics as Antitumor Agents*; Borders, D. B., Doyle, T. W., Eds.; Marcel Decker: New York, 1995.

(4) Myers, A. G.; Cohen, S. B.; Tom, N. J.; Madar, D. J.; Fraley, M. E. *J. Am. Chem. Soc.* **1995**, *117*, 7574.

(5) Myers, A. G.; Fraley, M. E.; Tom, N. J.; Cohen, S. B.; Madar, D. J. *Chem. Biol.* **1995**, *2*, 33.

(6) Myers, A. G.; Kort, M. E.; Cohen, S. B.; Tom, N. J. *Biochemistry* **1997**, *36*, 3903.
(7) Wender, P. A.; Kelly, R. C.; Beckham, S.; Miller, B. L. *Proc. Natl. Acad. Sci. U.S.A.* **1991**, *88*, 8835.
(8) Ahlstrom, B.; Kraka, E.; Cremer, D. *Chem. Phys. Lett.* **2002**, *361*, 129.
(9) Tuttle, T.; Kraka, E.; Cremer, D. *J. Am. Chem. Soc.* **2005**, *127*, 9469.
(10) Gräfenstein, J.; Hjerpe, A. M.; Kraka, E.; Cremer, D. *J. Phys. Chem. A* **2000**, *104*, 1748.
(11) Kraka, E.; Cremer, D. *J. Comput. Chem.* **2001**, *22*, 216.
(12) Kraka, E.; Cremer, D. *J. Am. Chem. Soc.* **2000**, *122*, 8245.
(13) Kraka, E.; Cremer, D. *J. Mol. Struct. (THEOCHEM*) **2000**, *506*, 191.
(14) Kraka, E.; Cremer, D. *J. Am. Chem. Soc.* **1994**, *116*, 4929.
(15) Kraka, E.; Cremer, D. *Chem. Phys. Lett.* **1993**, *216*, 333.
(16) Sugiura, Y.; Shiraki, T.; Konishi, M.; Oki, T. *Proc. Natl. Acad. Sci. U.S.A.* **1990**, *87*, 3831.
(17) Cardozo, M. G.; Hopfinger, A. J. *Biopolymers* **1993**, *33*, 377.
(18) Cardozo, M. G.; Hopfinger, A. J. *Mol. Pharmacol.* **1991**, *40*, 1023.
(19) Langley, D. R.; Doyle, T. W.; Beveridge, D. L. *J. Am. Chem. Soc.* **1991**, *113*, 4395.
(20) Wender, P. A.; Zercher, C. K. *J. Am. Chem. Soc.* **1991**, *113*, 2311.
(21) Arakawa, T.; Kusakabe, T.; Kuwahara, J.; Otsuka, M.; Sugiura, Y. *Biochem. Biophys. Res. Commun.* **1993**, *190*, 362.
(22) Basak, A.; Bdour, H. M.; Shain, J. C.; Mandal, S.; Rudra, K. R.; Nag, S. *Bioorg. Med. Chem. Lett.* **2000**, *10*, 1321.
(23) Guo, Q.; Lu, M.; Shahrestanifar, M.; Sheardy, R. D.; Kallenbach, N. R. *Biochemistry* **1991**, *30*, 11735.
(24) Ichikawa, A.; Kuboya, T.; Aoyama, T.; Sugiura, Y. *Biochemistry* **1992**, *31*, 6784.
(25) Kusakabe, T.; Uesugi, M.; Sugiura, Y. *Biochemistry* **1995**, *34*, 9944.
(26) Lu, M.; Guo, Q.; Kallenbach, N. R. *J. Biomol. Struct. Dyn.* **1991**, *9*, 271.
(27) Unno, R.; Michishita, H.; Inagaki, H.; Suzuki, Y.; Baba, Y.; Jomori, T.; Nishikawa, T.; Isobe, M. *Bioorg. Med. Chem.* **1997**, *5*, 987.
(28) Senn, H. M.; Thiel, W. *Top. Curr. Chem.* **2007**, *268*, 173.
(29) Morris, G. M.; Goodsell, D. S.; Halliday, R. S.; Huey, R.; Hart, W. E.; Belew, R. K.; Olson, A. J. *J. Comput. Chem.* **1998**, *19*, 1639.
(30) Morris, G. M.; Goodsell, D. S.; Huey, R.; Olson, A. J. *J. Comput.-Aided Mol. Des.* **1996**, *10*, 293.
(31) Weiner, S. J.; Kollman, P. A.; Case, D. A.; Singh, U. C.; Ghio, C.; Alagona, G.; Profeta, S.; Weiner, P. *J. Am. Chem. Soc.* **1984**, *106*, 765.
(32) Binkley, J. S.; Pople, J. A.; Hehre, W. J. *J. Am. Chem. Soc.* **1980**, *102*, 939.
(33) Hariharan, P. C.; Pople, J. A. *Theor. Chim. Acta.* **1973**, *28*, 213.
(34) Becke, A. D. *J. Chem. Phys.* **1993**, *98*, 5648.
(35) Becke, A. D. *Phys. Rev. A* **1988**, *38*, 3098.
(36) Lee, C. T.; Yang, W. T.; Parr, R. G. *Phys. Rev. B* **1988**, *37*, 785.
(37) Hertwig, R. H.; Koch, W. *Chem. Phys. Lett.* **1997**, *268*, 345.
(38) Stephens, P. J.; Devlin, F. J.; Chabalowski, C. F.; Frisch, M. J. *J. Phys. Chem.* **1994**, *98*, 11623.
(39) Roth, W. R.; Hopf, H.; Horn, C. *Chem. Ber.* **1994**, *127*, 1765.
(40) Cornell, W. D.; Cieplak, P.; Bayly, C. I.; Gould, I. R.; Merz, K. M.; Ferguson, D. M.; Spellmeyer, D. C.; Fox, T.; Caldwell, J. W.; Kollman, P. A. *J. Am. Chem. Soc.* **1995**, *117*, 5179.
(41) *HyperChem*; Hypercube, Inc.: Gainesville, FL, 2002.
(42) Brooks, B. R.; Bruccoleri, R. E.; Olafson, B. D.; States, D. J.; Swaminathan, S.; Karplus, M. *J. Comput. Chem.* **1983**, *4*, 187.
(43) MacKerell, A. D.; Brooks, B. R.; Brooks, C. L., III; Nilsson, L.; Roux, B.; Won, Y.; Karplus, M. In *Encyclopedia of Computational Chemistry*; Schleyer, P. v. R., Ed.; Wiley: Chichester, 1998; Vol. 1, p 271.
(44) Foloppe, N.; MacKerell, A. D. *J. Comput. Chem.* **2000**, *21*, 86.
(45) MacKerell, A. D.; Banavali, N.; Foloppe, N. *Biopolymers* **2000**, *56*, 257.
(46) MacKerell, A. D.; Banavali, N. K. *J. Comput. Chem.* **2000**, *21*, 105.
(47) Jorgensen, W. L.; Chandrasekhar, J.; Madura, J. D.; Impey, R. W.; Klein, M. L. *J. Chem. Phys.* **1983**, *79*, 926.
(48) *ChemShell*, version 3.0a3; CCLRC Daresbury Laboratory: Cheshire, U.K., 2004.
(49) Sherwood, P.; de Vries, A. H.; Guest, M. F.; Schreckenbach, G.; Catlow, C. R. A.; French, S. A.; Sokol, A. A.; Bromley, S. T.; Thiel, W.; Turner, A. J.; Billeter, S.; Terstegen, F.; Thiel, S.; Kendrick, J.; Rogers, S. C.; Casci, J.; Watson, M.; King, F.; Karlsen, E.; Sjovoll, M.; Fahmi, A.; Schafer, A.; Lennartz, C. *J. Mol. Struct. (THEOCHEM*) **2003**, *632*, 1.
(50) Frisch, M. J.; Trucks, G. W.; Schlegel, H. B.; Scuseria, G. E.; Robb, M. A.; Cheeseman, J. R.; Montgomery, J. J. A.; Vreven, T.; Kudin, K. N.; Burant, J. C.; Millam, J. M.; Iyengar, S. S.; Tomasi, J.; Barone, V.; Mennucci, B.; Cossi, M.; Scalmani, G.; Rega, N.; Petersson, G. A.; Nakatsuji, H.; Hada, M.; Ehara, M.; Toyota, K.; Fukuda, R.; Hasegawa, J.; Ishida, M.; Nakajima, T.; Honda, Y.; Kitao, O.; Nakai, H.; Klene, M.; Li, X.; Knox, J. E.; Hratchian, H. P.; Cross, J. B.; Bakken, V.; Adamo, C.; Jaramillo, J.; Gomperts, R.; Stratmann, R. E.; Yazyev, O.; Austin, A. J.; Cammi, R.; Pomelli, C.; Ochterski, J. W.; Ayala, P. Y.; Morokuma, K.; Voth, G. A.; Salvador, P.; Dannenberg, J. J.; Zakrzewski, V. G.; Dapprich, S.; Daniels, A. D.; Strain, M. C.; Farkas, O.; Malick, D. K.; Rabuck, A. D.; Raghavachari, K.; Foresman, J. B.; Ortiz, J. V.; Cui, Q.; Baboul, A. G.; Clifford, S.; Cioslowski, J.; Stefanov, B. B.; Liu, G.; Liashenko, A.; Piskorz, P.; Komaromi, I.; Martin, R. L.; Fox, D. J.; Keith, T.; Al-Laham, M. A.; Peng, C. Y.; Nanayakkara, A.; Challacombe, M.; Gill, P. M. W.; Johnson, B.; Chen, W.; Wong, M. W.; Gonzalez, C.; Pople, J. A. *Gaussian 03*, Revision C.01; Gaussian, Inc.: Wallingford, CT, 2004
(51) Bakowies, D.; Thiel, W. *J. Phys. Chem.* **1996**, *100*, 10580.
(52) Clark, T.; Chandrasekhar, J.; Spitznagel, G. W.; Schleyer, P. V. *J. Comput. Chem.* **1983**, *4*, 294.
(53) Gräfenstein, J.; Kraka, E.; Cremer, D. *Phys. Chem. Chem. Phys.* **2004**, *6*, 1096.
(54) Gräfenstein, J.; Kraka, E.; Cremer, D. *J. Chem. Phys.* **2004**, *120*, 524.
(55) Polo, V.; Gräfenstein, J.; Kraka, E.; Cremer, D. *Theor. Chem. Acc.* **2003**, *109*, 22.
(56) Polo, V.; Gräfenstein, J.; Kraka, E.; Cremer, D. *Chem. Phys. Lett.* **2002**, *352*, 469.
(57) Polo, V.; Kraka, E.; Cremer, D. *Mol. Phys.* **2002**, *100*, 1771.
(58) Polo, V.; Kraka, E.; Cremer, D. *Theor. Chem. Acc.* **2002**, *107*, 291.